Vibrational Dynamics of Poly(L-glutamine)

Sanjeev John La'Verne,[1] Shweta Srivastava,[2] Seema Srivastava,[2] V. D. Gupta[2]

[1]*Physics Department, Lucknow Christian College, Lucknow 226018, India*
[2]*Physics Department, Integral University, Lucknow 226026, India*

Received 4 September 2008; accepted 10 December 2008
DOI 10.1002/app.29995
Published online 14 April 2009 in Wiley InterScience (www.interscience.wiley.com).

ABSTRACT: In the present paper, we report the Fourier transform infra-red (FTIR) spectra and an analysis of the normal modes and their dispersion, based on the calculations for an infinite chain and Urey Bradley force field with nonbonded interactions. The results thus obtained agree well with the FTIR spectra. The heat capacity obtained from the dispersion curves via density-of-states is in very good agreement with the experimental measurements between 50 and 500 K. We observed that the main contribution to heat capacity comes from the modes involving the coupling of the backbone skeletal and side-chain motions. © 2009 Wiley Periodicals, Inc. J Appl Polym Sci 113: 1406–1414, 2009

Key words: poly(L-glutamine); heat capacity; density-of-states; dispersion curves

INTRODUCTION

Earlier, we reported the vibrational dynamics of biopolymeric systems having α, β, ω, and threefold helical conformations.[1–11] In continuation of these studies, we report on the vibration dynamics and heat capacity of poly(L-glutamine). These calculations were found to be in good agreement with the experimental measurements reported by Wunderlich et.al.[12–15] In most cases, their analysis is based on separation of the vibrational spectrum into group and skeletal vibrations. The former are taken from computationally fitted i.r. and Raman data and the latter by using the two-parameter Tarasov model[12] and fitting to low-temperature heat capacities. We also must carry out a complete normal-mode analysis to further study vibrational dynamics, including the heat capacity. The assignments of normal-mode frequencies are made on the basis of potential energy distribution (PED), which, together with line shape, line intensity, and the presence/absence of the modes in the molecule having atoms placed in similar environment. Furthermore, the dispersion curves provide knowledge of the degree of coupling and the dependence of the frequency of a given mode on the sequence length of ordered conformation. These curves also facilitate a correlation of the microscopic properties, such as specific heat, enthalpy, and free energy.

Correspondence to: V. D. Gupta (vdgupta24@rediffmail.com).

Journal of Applied Polymer Science, Vol. 113, 1406–1414 (2009)

Poly(L-glutamine) (PLGn) is a polypeptide with a glutamine side chain. It belongs to the class of poly (amino acids) having bulky hydrophobic side chains. Glutamine is a "nonessential" amino acid. It is found in the skeletal muscle, with the remainder residing in the lungs, liver, and stomach. Glutamine has a unique molecule structure with two nitrogen side chains. This makes glutamine the primary transporter of nitrogen in the muscle cells. The cells in the immune system rely on glutamine as their primary fuel source. The human body uses glutamine to move ammonia and nitrogen throughout the body via the bloodstream. Glutamine supplement is necessary after an intense training period. Glutamine is mostly tasteless.[16]

THEORETICAL APPROACH

Normal mode calculation

The calculation of normal mode frequencies has been carried out according to the well-known Wilson's GF[17] matrix method, as modified by Higgs.[18] It consists of writing the inverse kinetic energy matrix G and the potential energy matrix F in terms of internal coordinates R. In the case of an infinite isolated helical polymer, there are an infinite number of internal coordinate that lead to G and F matrices of infinite order. Due to the screw symmetry of the polymer, a transformation similar to that given by Born and Von Karman can be performed that reduces the infinite problem to finite dimensions.[19] The vibrational secular equation, which gives normal mode frequencies and their dispersion as a function of phase angle, has the form:

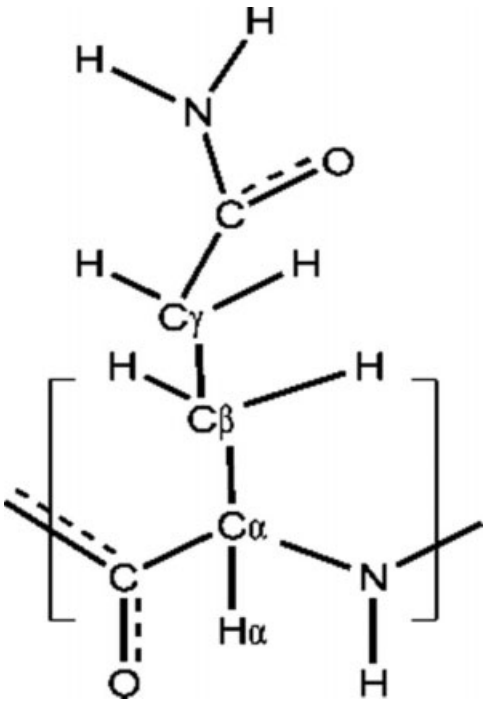

Figure 1 Chemical repeat unit of poly(L-glutamine).

$$G(\delta)F(\delta) - \lambda(\delta)I = 0, \quad 0 \le \delta \le \pi \tag{1}$$

The vibrational frequencies $\nu(\delta)$ (in cm^{-1}) are related to the eigenvalues $\lambda(\delta)$ by the following relation:

$$\lambda(\delta) = 4\pi^2 c^2 \nu^2(\delta) \tag{2}$$

where c is the velocity of light.

Calculation of specific heat

Dispersion curves can be used to calculate the specific heat of a polymeric system. For a one-dimensional system, the density-of-state function or the frequency distribution function expresses the way energy is distributed among various branches of normal modes in the crystal. It is calculated from the relation:

$$g(\nu) = \sum_j (\partial \nu_j / \partial \delta)^{-1}|_{\nu j(\delta) - \nu} \tag{3}$$

with $\int g(\nu_j)\, d\nu_j = 1$.

The sum if over all branches j. Considering a solid as an assembly of harmonic oscillators, the frequency distribution g(ν) is equivalent to a partition function. The constant volume heat capacity C_ν can be calculated using Debye's relation:

$$C_\nu = \sum_j g(\nu_j) k N_A (h\nu_j/kT)^2 \frac{\exp(h\nu_j/kT)}{[\exp(h\nu_j)/kT - 1]^2} \tag{4}$$

where $g(\nu)$ is density of states; k is Boltzmann constant; N is Avogadro number; T is absolute temperature; and h is Planck's constant.

The constant volume heat capacity C_ν, given by eq. (4), is converted into constant pressure heat capacity C_p, using the Nernst-Lindemann approximation.[19,20]

$$C_p - C_\nu = 3RA_0(C_p^2 T / C_\nu T_m^0) \tag{5}$$

where A_0 is a constant often of a universal value [3.9×10^{-9} (kmol/J)] and T_m^0 is the equilibrium melting temperature.

RESULTS AND DISCUSSIONS

The FTIR spectra (Fig. 2) were obtained on a Perkin Elmer model RX-1. The spectrograph was purged with liquid nitrogen before taking the spectra. Poly(L-glutamine) is α-helical in form. There are 17 atoms per residue unit (Fig. 1) that gives rise to 51 dispersion curves. The Urey Bradley force constants were initially transferred from the earlier work on poly(L-leucine)[21] and were further refined by using the least-squares fit method. Final set of force constants for poly(L-glutamine) are given in Table I. The vibrational frequencies were calculated for values of δ varying from 0 to π in steps of 0.05 π. Assuming that ψ is the angle of rotation about the helix axis that separates the adjacent units, the modes corresponding to $\delta = 0$ (A species) and ψ (E species) are infra-red active and corresponding to $\delta = 0$, ψ, 2ψ (E species) are Raman active modes. The four zero frequencies correspond to acoustic modes, three representing translations along the three axes, and one is rotation around the chain axis. The assignments have been made on the basis of potential energy distribution, band position, band shape, band intensity, derivative spectra, and absorption/scattering in similar molecules having groups placed in similar environments. Full use has been made of the spectral information available in Refs. 2 and 3 and Ref. 11. Except for a couple of frequencies, most of the frequencies are fitted within less than 1%. As mentioned earlier, the modes corresponding to $\delta = 0.0$ are both Raman and IR active. Therefore, the calculated frequencies are first fitted to the observed frequencies for this phase value. For the sake of simplicity, it is convenient to discuss the normal frequencies under two separate heads, viz., amide modes, side chain modes, and mixed mode. All amide modes, side chain modes, and mixed modes, along with their potential energy distribution, are given in Tables II–IV, respectively. Table V shows the comparison of the amide modes of α-helical polypeptides.

The significant contribution from a force constant is taken to be 5%. The calculated frequencies are compared with the observed ones. Since the modes above 1350 cm^{-1} are nondispersive, only the modes below this are shown in Figures 3(a), 4(a), and 5(a). Figure 6 shows the variation of heat capacity with temperature.

TABLE I
Internal Coordinates and Force Constants (md/Å)[a]

1	ν(N—H)	5.39
2	ν(N—Cα)	3.10
3	ν(Cα—C)	2.80
4	ν(C=O)	8.50
5	ν(Cα—Ha)	5.10
6	ν(Cα—Cβ)	3.40
7	ν(Cβ—Hb)	4.55
8	ν(Cβ—Cγ)	2.90
9	ν(Cγ—Hg)	4.50
10	ν(Cγ—C)	2.25
11	ν(C=O)s	9.70
12	ν(C—N)s	4.20
13	ν(N—H)s	5.395
14	ν(C=N)	6.50
15	Φ(H—N—Cα)	0.462 (0.60)
16	Φ(N—Cα—Ha)	0.23 (0.60)
17	Φ(N—Cα—C)	0.45 (0.50)
18	Φ(N—Cα—Cβ)	0.42 (0.50)
19	Φ(H—Cα—C)	0.410 (0.18)
20	Φ(Cβ—Cα—Cβ)	0.52 (0.18)
21	Φ(Ha—Cα—Cβ)	0.26 (0.20)
22	Φ(Cα—C=O)	0.21 (0.60)
23	Φ(Cα—C=N)	0.21 (0.50)
24	Φ(N=C=O)	0.65 (0.90)
25	Φ(Cα—Cβ—Hb)	0.45 (0.20)
26	Φ(Cα—Cβ—Cγ)	0.52 (0.18)
27	Φ(Hb—Cβ—Cγ)	0.42 (0.20)
28	Φ(Hb—Cβ—Hb)	0.375 (0.24)
29	Φ(Cβ—Cγ—Hg)	0.447 (0.20)
30	Φ(Cβ—Cγ—C)	0.52 (0.18)
31	Φ(Hg—Cγ—C)	0.46 (0.20)
32	Φ(Hg—Cγ—Hg)	0.33 (0.24)
33	Φ(Cγ—C=O)s	0.23 (0.60)
34	Φ(Cγ—C—N)s	0.20 (0.50)
35	Φ(N—C=O)s	0.65 (0.40)
36	Φ(C—N—H)s	0.285 (0.60)
37	Φ(H—N—H)s	0.205 (0.40)
38	Φ(C=N—H)	0.23 (0.65)
39	Φ(C=N—C)	0.53 (0.35)
40	ω(Cα—Ha)	0.14
41	ω(C=O)	0.535
42	ω(Cβ—Hb)	0.18
43	ω(Cγ—Hg)	0.17
44	ω(C=O)s	0.54
45	ω(N—H)s	0.095
46	ω(N—H)	0.13
47	τ(Cα—C)	0.16
48	τ(Cα—Cβ)	0.16
49	τ(Cβ—Cγ)	0.16
50	τ(Cγ—C)	0.16
51	τ(C—N)s	0.010
52	τ(C=N)	0.035
53	τ(N—Cα)	0.010

[a] ν, ϕ, ω, and τ denote stretch, angle bend, wag, and torsion, respectively. Nonbonded force constants are given in parentheses.

Backbone and mixed modes

The main chain of poly(L-glutamine) PLGn consists of amide group joined together by Cα atoms. Modes involving the motions of main chain atoms (C—Cα—N) are termed as backbone modes. Pure backbone modes are given in Table II and pure side chain modes in Table III. The modes involving the coupling of backbone and side chains are given in Table IV. A comparison of various amide modes of αPLGn with αPoly(L-leucine)[21] and αPoly(L-alanine)[8] is given in Table V. Amide I, II, and III modes fall nearly in the same region. It is clear that the frequency of amide V mode does not depend solely on the main-chain conformation, but side chain structure also plays an important role in determining the frequency of these modes. These modes mix strongly and very differently with the side chain coordinates, depending on the structure of the main and side chains.

In FTIR of PLGn (Fig. 2), the amide A mode is observed at 3321 cm^{-1}, which is calculated at 3318 cm^{-1}. This value is almost conformation dependent. In α-helical poly(γ-benzyl-L-glutamate),[22] the amide A frequency is observed at 3300 cm^{-1}. In the present work, the amide I and amide II modes of PLGn are observed in FTIR (Fig. 2) at 1687 and 1587 cm^{-1}, respectively. The corresponding calculated values are 1683 and 1591 cm^{-1}. These frequencies are in the characteristic region of the modes for α-helical structures, e.g., the amide I and amide II modes for poly(γ-benzyl-L-glutamate)[22] and poly(L-leucine)[21] have been reported at 1653 and 1550, and 1650 and 1540 cm^{-1}, respectively.

It is observed that amide III vibrations are rather complicated, involving a number of stretching and deformation modes of the amide group. In addition, it may contain some (Cα—C) stretch mixed with it. In the present case also, this vibration is not isolated within the peptide group and we see that it appears at 1317 cm^{-1}, matching well with the calculated values 1313 cm^{-1}. This also agrees well with the amide III band reported at 1299, 1298, and 1313 cm^{-1} in poly(L-leucine),[21] poly(β-benzyl-L-aspartate),[1] and poly(α-amino isobutyric acid),[23] which show α-helical structure. The amide IV is observed at 480 cm^{-1} and is calculated at 488 cm^{-1}. In poly(L-histidine) under study, it was calculated at 486 cm^{-1}.

In addition to in-plane modes of CO—NH group discussed above, there are three out-of-plane vibrations. The amide V and amide VI are due to NH and C=O out-of-plane wagging modes, and the amide VII is due to internal rotation about the CN bond. The amide V mode is observed at 539 cm^{-1} and it is matched to the calculated frequency at 535 cm^{-1}. CO wag and NH wag are the main components of this mode. In poly(L-glutamic acid),[3] the amide V band appears at 552 cm^{-1}. The amide VI mode is observed at 777 cm^{-1} and is calculated at 776 cm^{-1}. This amide mainly consists of CO wag and NH wag. In poly(L-tyrosine)[24] and poly(L-histidine) under study it was observed at 766 cm^{-1}.

The amide VII mode has been calculated at 194 cm^{-1}. This vibration, mainly a CN torsion mode of

TABLE II
Pure Backbone Modes

Calc	Obs	Assignments (%PED at $\delta = 0.0$)
3318	3321	ν(N—H) (100) **AMIDE A**
1683	1687	ν(C=O) (54) + ν(C=N) (35) **AMIDE I**
1591	1587	φ(H—N—Cα) (43) + φ(C=N—H) (28) + ν(C=N) (12) **AMIDE II**
1313	1317	ν(C=N) (27) + ν(Cα—C) (17) + ν(C=O) (13) + φ(H—N—Cα) (9)+ φ(N=C=O) (8) + φ(N—Cα—Hα) (6) **AMIDE III**
897	897	ν(Cα—C)(21) + φ(N=C=O)(14) + φ(C=N—C)(11) + ν(C=O) (10) + ν(C=N) (7)
776	777	ω(C=O) (41) + ω(N—H) (32) + τ(C=N) (12) **AMIDE VI**
Cal.	Obs.	Assignments (% PED at $\delta = 5\pi/9$)
3318	3321	ν(N—H) (99) **AMIDE A**
1682	1687	ν(C=O) (54) + ν(C=N) (35) **AMIDE I**
1582	1587	φ(H—N—Cα)(44) + φ(C=N—H) (29) + ν(C=N) (10) **AMIDE II**
1357	1317	ν(Cα—C) (14) + ν(C=N) (14) + ν(N—Cα) (14) + φ(N—Cα—Hα) (14)+ ν(C=O) (7) + φ(H—N—Cα) (5) **AMIDE III**
896	897	ν(Cα—C) (25) + ν(Cα—Cβ) (8) + φ(N=C=O) (8) + ν(N—Cα) (6)+ ν(C=O) (6)
799	777	ω(C=O)(33) + ω(N—H)(24)+ τ(C=N)(9)+ ν(Cγ—C)(7)+ ν(Cα—Cβ)(7)+ φ(N—Cα—C) (5) **AMIDE VI**

Note: All frequencies are in cm^{-1}.

the peptide link, is theoretically important because of its direct relation to the potential barrier hindering internal rotation and is specific to the position of CO and NH bands relating to one another. In poly(L-histidine) under study, the amide VII mode was calculated at 180 cm^{-1}.

Side chain modes

Strong lines calculated at 1637 cm^{-1} observed at 1639 cm^{-1} were assigned to the CO stretching in the side chain of poly(L-glutamine). Andreas Barth[24] has bands at 1668 cm^{-1}. He has also assigned CN stretching at 1084 cm^{-1}, which was observed at 1107 cm^{-1}, calculated at 1105 cm^{-1}.

The conformation-insensitive CH_2 scissoring mode in the side chain, calculated at 1465 cm^{-1}, was observed at 1462 cm^{-1}; this has been observed at nearly the same value at 1449 cm^{-1} in poly(L-leucine),[21] 1453 cm^{-1} in poly(γ-benzyl-glutamate),[22] and at 1450 cm^{-1} in poly(L-glutamic acid).[3] The above modes are localized modes and nondispersive in nature.

Dispersion curves

In the region below 1350 cm^{-1}, the modes are mostly coupled, and, depending on the degree of coupling, conformation, and chemical species, show some characteristic features. Some of the modes exhibiting special features are discussed below.

As seen for the 816 cm^{-1} mode and the 776 cm^{-1} mode, there is attraction between them with an increase in delta value, as shown in Table VI. We see that for the 816 cm^{-1} mode, this is due to

TABLE III
Pure Side Chain Modes

Calc	Obs.	Assignments (% PED at $\delta = 0$)
3324	3321	ν(N—H) (100)
3266	3270	ν(N—H) (100)
3179	3175	ν(Cα—Hα) (100)
2994	2987	ν(Cβ—Hβ) (96)
2978	2987	ν(Cγ—Hγ) (95)
2974	2957	ν(Cβ—Hβ) (99)
2958	2957	ν(Cγ—Hγ) (99)
1639	1637	ν(C=O) (85) + ν(Cγ—C) (5)
1480	1488	φ(H—N—H) (54) + φ(C—N—H) (43)
1410	1412	φ(Hγ—Cγ—Hγ) (62) + φ(Cβ—Cγ—Hγ) (16) + ω(Cγ—Hγ) (12)
1107	1105	φ(C—N—H) (47) + φ(Hγ—Cγ—C) (11) + ν(C—N)s (8)
954	945	ν(Cβ—Cγ) (52) + ω(N—H) (8) + φ(Hβ—Cβ—Cγ) (8) + φ(Cβ—Cγ—Hγ) (7)
925	926	ω(N—H) (84) + ν(Cβ—Cγ) (8)
857	849	φ(Hβ—Cβ—Cγ) (18) + ω(Cβ—Hβ) (16) + φ(Cβ—Cγ—Hγ) (14) + ω(Cγ—Hγ) (14)+ φ(Hγ—Cγ—C) (8) + φ(Cα—Cβ—Hβ) (7)
447	456	φ(N—C=O) (89)
105	–	τ(C—N) (91)

Note: All frequencies are in cm^{-1}.

TABLE IV
Mixed Modes

Calc	Obs.	Assignments (% PED at $\delta = 0$)	Calc	Obs.	Assignments (% PED at $\delta = 5\pi/9$)
1465	1462	ϕ (Hβ—Cβ—Hβ) (62) + ϕ(Cα—Cβ—Hβ) (16) + ω(Cβ—Hβ) (11) + ν(Cα—Cβ) (5)	1465	1462	ϕ (Hβ—Cβ—Hβ)(61)+ϕ(Cα—Cβ—Hβ)(16)+ ω(Cβ—Hβ)(11)+ ν(Cα—Cβ)(6)
1367	1359	ϕ(N—Cα—Hα) (22) + ν(Cα—Cβ)(17) + ϕ(Hα—Cα—Cβ) (13)+ ϕ(Hβ—Cβ—Cγ) (9) + ω(Cα—Hα) (6) + ν(Cβ—Cγ) (6)	1369	1359	ν(Cα—Cβ)(17)+ϕ(N—Cα—Hα)(14)+ϕ(Hβ—Cβ—Cγ)(11)+ ϕ(Hα—Cα—Cβ)(9) ν(Cβ—Cγ) (7) + ν(Cα—C) (5) + ϕ(Hγ—Cγ—C) (5)
1336	1334	ϕ(Hγ—Cγ—C) (12) + ϕ(N—Cα—Hα) (12) + ϕ(Hβ—Cβ—Cγ) (11) + ν(Cβ—Cγ)(10)+ ϕ(Cα—Cβ—Hβ) (8) + ϕ(Cβ—Cγ—Hγ) (7) + ν(N—Cα) (7) + ν(C=O) (5)	1321	1334	ϕ(Hγ—Cγ—C)(17)+ϕ(N—Cα—Hα)(12)+ϕ(Cβ—Cγ—Hγ)(10)+ ν(Cβ—Cγ) (9) ν(C=N) (7)+ϕ(Hβ—Cβ—Cγ)(7)+ ν(Cγ—C)(6)+ ν(Cα—C) (5)
1263	1257	ϕ(Hγ—Cγ—C) + ϕ(Cβ—Cγ—Hγ) (13) + ϕ(Cα—Cβ—Hβ) (11) + ϕ(Hβ—Cβ—Cγ) (10)+ ν(C—N)s (8) + ν(Cγ—C) (7) + ν(Cα—C) (6) + ν(Cα—Cβ) (6)	1253	1257	ϕ(Hγ—Cγ—C)(20)+ϕ(Hβ—Cβ—Cγ)(15)+ϕ(Cα—Cβ—Hβ)(13)+ ν(C—N)s(11) ϕ(Cβ—Cγ—Hγ) (10) + ν(Cγ—C) (6) + ν(Cα—Cβ) (6)
1224	1230	ν(C—N)s (43) + ϕ(Hγ—Cγ—C) (23) + ϕ(Cβ—Cγ—Hγ) (7) + ϕ(Cα—Cβ—Hβ) (5)	1221	1230	ν(C—N)s (46) + ϕ(Hγ—Cγ—C) (28) + ϕ(Cβ—Cγ—Hγ) (8)
1206	1203	ϕ(Cα—Cβ—Hβ) (20) + ν(N—Cα) (19) + ν(C—N)s (9) + ϕ(Hβ—Cβ—Cγ) (8)+ ν(Cα—C) (8) + ϕ(Hγ—Cγ—C) (7) + ω(Cβ—Hβ) (5)	1196	1203	ϕ(Cα—Cβ—Hβ) (24)+ ν(N—Cα) (20)+ω(Cβ—Hβ)(7)+ϕ(Cβ—Cγ—Hγ) (6) ϕ(Cβ—Cγ—Hγ) (6)
1154	1164	ϕ(Cβ—Cγ—Hγ) (37) + ϕ(Hβ—Cβ—Cγ) (24) + ϕ(H—Cα—C) (12) + ω(Cγ—Hγ) (7)	1154	1164	ϕ(Cβ—Cγ—Hγ)(33)+ϕ(Hβ—Cβ—Cγ)(24)+ϕ(H—Cα—C)(15)+ω(Cγ—Hγ)(6)
1137	1132	ϕ(H—Cα—C) (39) + ϕ(Hβ—Cβ—Cγ) (16) + ϕ(Cα—Cβ—Hβ) (12) + ν(Cα—Cβ) (6)+ ϕ(Hα—Cα—Cβ) (5)	1140	1132	ϕ(H—Cα—C)(33)+ϕ(Hβ—Cβ—Cγ)(17)+ϕ(Cα—Cβ—Hβ)(12)+ ν(Cα—Cβ) (7) ϕ(Cβ—Cγ—Hγ) (6)
1078	1086	ϕ(C—N—H)s (29) + ϕ(Hβ—Cβ—Cγ) (15)+ ν(N—Cα) (14)+ϕ(Cα—Cβ—Hβ) (13)+ ϕ(Cβ—Cγ—Hγ) (6) + ν(C—N)s (5) + ϕ(Hγ—Cγ—C) (5)	1077	1086	ϕ(C—N—H)s (27)+ϕ(Hβ—Cβ—Cγ)(15)+ ν(N—Cα)(15)+ϕ(Cα—Cβ—Hβ)(12) ϕ(Cβ—Cγ—Hγ) (5)
1032	1052	ν(Cα—Cβ) (22) + ϕ(Hγ—Cγ—C) (15) + ϕ(Cα—Cβ—Hβ) (12) + ν(C—N)s (10)+ ϕ(Hα—Cα—Cβ) (8) + ω(Cβ—Hβ) (6)	1041	1052	ν(Cα—Cβ)(17)+ϕ(Hγ—Cγ—C)(15)+ ν(C—N)s (10)+ϕ(Hα—Cα—Cβ) (10) ϕ(H—Cα—C) (9) + ϕ(Cα—Cβ—Hβ) (9)
1001	999	ν(Cα—Cβ) (14) + ϕ(Cα—Cβ—Hβ) (13) + ν(Cα—C) (12) + ϕ(Hγ—Cγ—C) (10)+ ϕ(H—Cα—C) (9) + ν(N—Cα) (8) + ϕ(Hα—Cα—Cβ) (7) + ω(Cγ—Hγ) (5)	993	999	ϕ(Cα—Cβ—Hβ) (12)+ϕ(Hγ—Cγ—C) (12)+ ν(N—Cα) (11)+ ν(Cα—C) (8) ν(Cα—Cβ) (7)+ω(Cγ—Hγ) (7)+ϕ(Hα—Cα—Cβ) (6)+ϕ(H—Cα—C)(5)
816	810	ν(Cγ—C)67)+ϕ(Cα—Cβ—Cγ)(5)	815	810	ν(Cγ—C) (61)
654	653	ϕ(N—Cα—C) (18) + ω(N—H) (9) + ω(C=O)s (9) + ϕ(Cγ—C=O)s (7)+ ω(C=O) (6) + ϕ(Cα—Cβ—Cγ) (5) + ϕ(Cβ—Cγ—C) (5)	622	621	ω (C=O)s (20)+ϕ(Cγ—C=O)s (15)+ϕ(N=C=O) (10) ν(Cβ—Cγ) (8)+ϕ(Cβ—Cγ—C)(7)
592	598	ω(C=O)s (27) + ϕ(Cγ—C=O)s (20) + ω(C=O) (9) + ϕ(N—Cα—C) (8)+ϕ(Cβ—Cγ—C) (5)	597	598	ϕ(N=C=O) (17)+ω(C=O)s (11)+ϕ(Cγ—C=O)s (8)+ϕ(Cβ—Cα—Cβ)(7) ω(C=O) (7) + ω(N—H) (6)
535	539	ω(N—H) (23) + ω(C=O) (15) + ν(N—Cα) (9) + ϕ(N=C=O) (9) + τ(C=N) (8)+ ϕ(Cβ—Cα—Cβ) (8) + ϕ(Cα—Cβ—Cγ) (6) **AMIDE V**	560	539	ω(N—H)(35)+ω(C=O)(26)+ τ(C=N)(9)+ϕ(N—Cα—C)(7) ω(C=O)s (6) **AMIDE V**
488	480	ϕ(Cα—C=O) (22) + ϕ(Cα—C=N) (22) + ϕ(N—Cα—Cβ) (15) + ϕ(Hα—Cα—Cβ) (9) **AMIDE IV**	434	413	ϕ(Cα—C=O)(17)+ϕ(Cα—C=N)(12)+ϕ(N—Cα—Cβ)(9)+ϕ(Hα—Cα—Cβ)(9) ϕ(N—C=O)s (8) + ϕ(N—Cα—C) (7) **AMIDE IV**
319	–	ϕ(Cγ—C—N)s (28) + ϕ(N=C=O) (12) + ϕ(C=N—C) (9) + ϕ(Cα—C=O) (9)+ ϕ(Cβ—Cα—Cβ) (9) + ω(C=O) (7) + ϕ(Cβ—Cγ—C) (6)	337	–	ϕ(C=N—C)(12)+ϕ(N=C=O)(11)+ϕ(N—Cα—C)(11)+ϕ(N—Cα—Cβ)(10) ω(C=O) (9)+ϕ(Cα—C=O) (6)+ϕ(Cα—Cβ—Cγ) (5)
301	–	ϕ(Cγ—C—N)s (48) + ϕ(N=C=O) (13) + ϕ(Cα—Cβ—Cγ) (6) + ϕ(Cα—C=O) (5)	304	–	ϕ(Cγ—C—N)s (72)
253	–	ϕ(Cβ—Cα—Cβ) (30) + ϕ(N—Cα—Cβ) (15) + ϕ(Cγ—C—N)s (9) + ω(C=O) (6)+ ϕ(Cβ—Cγ—C) (6)	271	–	ϕ(N—Cα—Cβ)(27)+ϕ(Cβ—Cα—Cβ)(18)+ ϕ(Cα—C=O) (8)+ ϕ(Cγ—C—N)s (5)
194	–	ϕ(N—Cα—C) (40) + ϕ(N—Cα—Cβ) (9) + ϕ(Cβ—Cγ—C) (8) + τ(C=N) (6)+ ϕ(Cα—C=N) (5) **AMIDE VII**	185	–	ϕ(Cα—Cβ—Cγ) (33) + ϕ(N—Cα—C) (18) + ϕ(Cγ—C—N)s (6)
151	–	ϕ(Cα—Cβ—Cγ) (24) + ϕ(Cβ—Cγ—C) (8) + ϕ(Cα—C=N) (8)+ ν(Cα—C) (7) + ν(Cα—Cβ) (6) + ϕ(C=N—C) (5)	162	–	ϕ(Cβ—Cγ—C) (34) + ϕ(C=N—C) (7) + ϕ(Cα—C=O) (6)+ ϕ(Cα—Cβ—Cγ) (5)
131	–	ϕ(Cβ—Cγ—C) (23) + ϕ(C=N—C) (13) + ϕ(N—Cα—Cβ) (10) + ϕ(Cα—Cβ—Cγ) (8)+ ϕ(Cα—C=N) (6) + τ(C—N)s (5)	121	–	ϕ(C=N—C)(21)+ϕ(Cα—C=N)(16)+ϕ(N—Cα—C)(9)+ϕ(N—Cα—Cβ)(9)+ ϕ(N=C=O)(8)+ϕ(C=N—H) (6)+ τ(C=N)(5)
79	–	ϕ(Cβ—Cα—Cβ) (19) + ϕ(Cα—Cβ—Cγ) (12) + ϕ(C=N—C) (9) + ϕ(Cβ—Cγ—C) (8)+ τ(Cα—Cβ) (8) + ϕ(Cα—C=N) (6) + τ(Cγ—C) (5)	78	–	ϕ(Cβ—Cα—Cβ)(28)+ϕ(Cβ—Cγ—C)(13)+ϕ(Cα—Cβ—Cγ)(10)+ ω(C=O)(6)
43	–	τ(Cγ—C) (59) + τ(Cβ—Cγ) (11) + τ(Cα—Cβ) (8)	47	–	τ(Cγ—C) (64)+ τ(Cα—Cβ) (17)+ τ(Cβ—Cγ) (7)
26	–	τ(Cα—C) (46) + τ(N—Cα) (34)	27	–	τ(N—Cα) (24)+ τ(Cα—C) (20)+ τ(Cβ—Cγ) (16)+ τ(Cα—Cβ)(14)
18	–	τ(Cα—Cβ) (60) + τ(Cγ—C) (24) + τ(Cβ—Cγ) (11)	16	–	τ(Cα—Cβ) (36) + τ(Cβ—Cγ) (34) + τ(Cγ—C) (22)
11	–	τ(Cβ—Cγ) (65) + τ(Cα—Cβ) (15)	12	–	τ(Cβ—Cγ) (28) + τ(Cα—Cβ) (21) + τ(Cα—C) (18) + τ(C=N) (8)

Note: All frequencies are in cm^{-1}.

TABLE V
Comparison of Amide Modes of α-Helical Polypeptides

	Poly(L-glutamine)	Poly(L-leucine)	Poly(L-alanine)
AMIDE A	3,318	3,313	3,293
AMIDE I	1,683	1,657	1,659
AMIDE II	1,591	1,546	1,515
AMIDE III	1,313	1,299	1,270
AMIDE IV	535	587	525
AMIDE V	488	587	595
AMIDE VI	776	656	685
AMIDE VII	194	216	238

stretching of (Cγ—C) and angle bend of (Cα—Cβ—Hβ).We see a variation in the above contributions with the change in the delta values; at $\delta = 0.20$, we see that contribution of (Cα—Cβ—Hβ) becomes zero. For the 776 cm^{-1} mode, we see at $\delta = 0.40$ contribution of stretching of (Cα—Cβ). At $\delta = 0.85$, it is seen that contribution of stretching of (Cγ—C) and stretching of (Cα—Cβ) becomes zero.

For the 653, 592, 535, and 488 cm^{-1} modes, it is observed for 653 cm^{-1}, at $\delta = 0.15$ angle bend of (Cα—Cβ—Cγ) becomes zero. Further, at $\delta = 0.20$, the contribution of angle bend of (N=C=O) becomes zero; contribution of stretching of (Cβ—Cγ) exists between $\delta = 0.25$ and 0.75.Contribution of wagging of (Cα—Hα) becomes zero at $\delta = 0.40$. It is observed at $\delta = 0.70$, contribution of angle bend of (C=N—C) and (Cβ—Cα—Cβ) comes in and contribution of angle bend of (Cβ—Cγ—C) becomes zero. At $\delta = 0.75$, contribution of angle bend of (Cγ—C=O) of the side chain becomes zero. For the 592 cm^{-1} mode, we see that at $\delta = 0.20$ contribution of angle bend of (Cβ—Cγ—C) becomes zero. For this mode there has been observed exchange of character with the 653 cm^{-1} mode; at $\delta = 0.70$ there is exchange of character for angle bend (Cβ—Cα—Cβ) and (Cβ—Cγ—C), as shown in Table VII. For the 535 cm^{-1} mode it is observed at $\delta = 0.15$ that the contribution of angle bend of (Cα—Cβ—Cγ) becomes zero, again exchange of character is seen between this mode and the 592 cm^{-1} mode for angle bend of (N=C=O) at $\delta = 0.40$, as shown in Table VII. Furthermore, for the 535 cm^{-1} mode at $\delta = 0.40$, the contribution of stretching of (N—Cα) becomes zero and at $\delta = 0.45$ the contribution of angle bend of (Cβ—Cα—Cβ) becomes zero. For the 488 cm^{-1} mode we see, at $\delta = 0.40$ the contribution of angle bend of (N—C=O) of the side chain comes in and at $\delta = 0.45$ there is exchange of character with the 447 cm^{-1} mode for the contribution of angle bend of (Hα—Cα—Cβ), as shown in Table VII. For the 447 cm^{-1} mode, which starts with purely the contribution of angle bend of (N—C=O) of the side chain, at $\delta = 0.45$ the contribution of angle bends of (Cα—C=O),(Cα—C=N), and (N—Cα—Cβ) comes in at $\delta = 0.60$; we see that the contribution of angle bend of (N—C=O) of the side chain becomes zero.

For the 131, 105, and 79 cm^{-1} modes, we observe for 131 cm^{-1} mode, at $\delta = 0.15$ the contribution of torsion of C—N of the side chain becomes zero and comes in back at $\delta = 0.75$. At $\delta = 0.45$, the

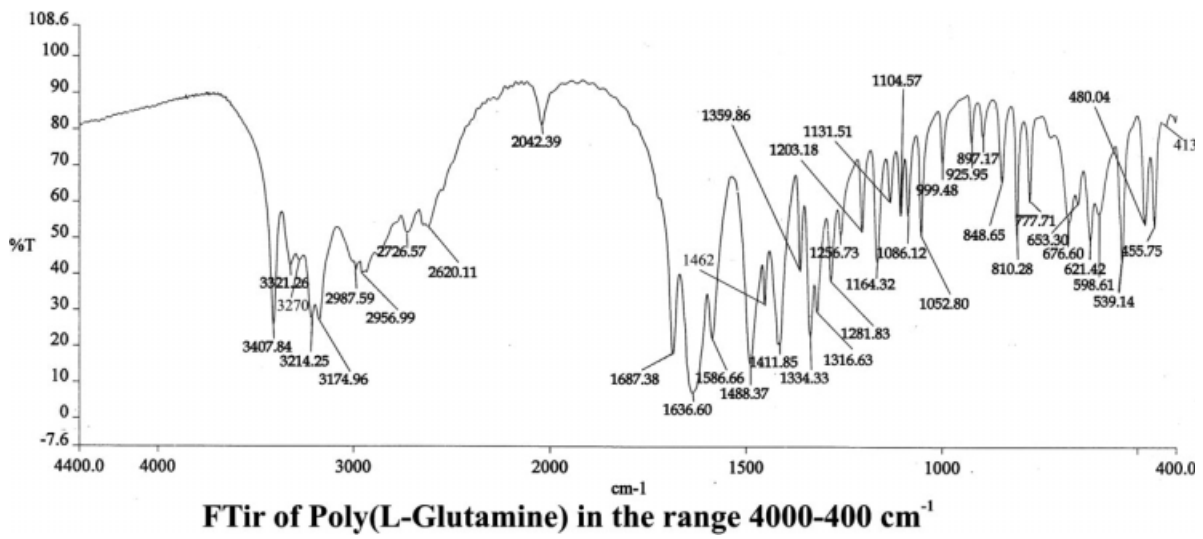

Figure 2 FTIR spectra of poly(L-glutamine).

TABLE VI
Pair of Modes that Exchange Character

Before exchange			After exchange		
Frequency	Delta	Assignments (% PED)	Frequency	Delta	Assignments (% PED)
619	0.65	ω(C=O)s(16)+ϕ(N=C=O)(15)+ϕ(Cγ—C=O)s(12) + ω(N—H)(6)+ ν(Cβ—Cγ)(6)+ϕ(Cβ—Cγ—C)(6)+ ν(Cα—C)(6)	621	0.70	ϕ(N=C=O)(19)+ω(N—H)(10)+ω(C=O)s(9)+ϕ(Cγ—C=O)s(7) + ν(Cα—C)(6)+ϕ(C=N—C)(6) +ϕ(Cβ—Cα—Cβ)(5)
607		ω(C=O)s(17)+ϕ(N=C=O)(15)+ϕ(Cγ—C=O)s(12) + ω(N—H)(7)+ϕ(Cβ—Cα—Cβ)(6)+ω(C=O)(6)	608		ω(C=O)s(24)+ϕ(Cγ—C=O)s(18)+ϕ(N=C=O)(12)+ ϕ(Cβ—Cγ—C)(6) + ν(Cβ—Cγ)(6)
635	0.35	ω(C=O)s(14)+ϕ(Cγ—C=O)s(11)+ϕ(N—Cα—C)(9) + ϕ(N=C=O)(7)+ω(N—H)(7)+ϕ(Cβ—Cγ—C)(6) + ν(Cβ—Cγ)(6)+ω(C=O)(5)	631	0.40	ω(C=O)s(16)+ϕ(Cγ—C=O)s(12)+ϕ(N=C=O)(8)+ ϕ(N—Cα—C)(7)+ϕ(Cβ—Cγ—C)(7)+ ν(Cβ—Cγ)(6) +ω(N—H)(6)
557		ω(N—H)(34)+ω(C=O)(21)+ τ(C=N)(9) + ϕ(Cβ—Cα—Cβ)(7)+ϕ(N=C=O)(7)	560		ω(N—H)(36)+ω(C=O)(23)+ τ(C=N)(10)+ϕ(Cβ—Cα—Cβ)(6)
456	0.40	ϕ(N—C=O)s(21)+ϕ(Cα—C=O)(16)+ϕ(Cα—C=N)(12) + ϕ(N—Cα—Cβ)(10)+ϕ(Hα—Cα—Cβ)(7)	452	0.45	ϕ(N—C=O)s(50)+ϕ(Cα—C=O)(10)+ϕ(Cα—C=N)(7)+ϕ(N—Cα—Cβ)(5)
445		ϕ(N—C=O)s(69)	443		ϕ(N—C=O)s(40)+ϕ(Cα—C=O)(10)+ϕ(Cα—C=N)(8) + ϕ(N—Cα—Cβ)(7)+ϕ(Hα—Cα—Cβ)(5)

Note: All frequencies are in cm^{-1}.

TABLE VII
Pair of Modes that Attract and Repel

Frequency	Delta	Assignments (% PED)	Frequency	Delta	Assignments (% PED)
777	0.10	ω(C=O)(40) + ω(N—H)(31) + τ(C=N)(12)	806	0.90	ω(C=O)(38) + ω(N—H)(24) + τ(C=N)(9) + ϕ(N—Cα—C)(6)
815		ν(Cγ—C)(67) + ϕ(Cα—Cβ—Cγ) (5)	812		ν(Cγ—C)(65)
301	0.10	ϕ(Cγ—C—N)s(50) + ϕ(N=C=O)(12) + ϕ(Cα—Cβ—Cγ)(6)	305	0.90	ϕ(Cγ—C—N)s(71) +ϕ(Cα—Cβ—Cγ)(5)
320		ϕ(Cγ—C—N)s(26) +ϕ(N=C=O)(12) + ϕ(C=N—C) (9) + ϕ(Cα—C=O)(9) + ϕ(Cβ—Cα—Cβ)(9) + ω(C=O)(7)+ ϕ(Cβ—Cγ—C)(6)	350		ϕ(N—Cα—Cβ)(22) + ϕ(C=N—C)(12) + ϕ(N—Cα—C)(10)+ ω(C=O)(9) + ν(Cα—C)(7) + ϕ(Cα—Cβ—Cγ)(6)
442	0.45	ϕ(N—C=O)s(40) + ϕ(Cα—C=O)(10) +ϕ(Cα—C=N)(8) + ϕ(N—Cα—Cβ)(7) + ϕ(Hα—Cα—Cβ)(5)	434	0.54	ϕ(Cα—C=O)(17) + ϕ(Cα—C=N)(12) +ϕ(N—Cα—Cβ)(9)+ ϕ(Hα—Cα—Cβ)(9) +ϕ(N—C=O)s(8) + ϕ(N—Cα—C)(7)
451		ϕ(N—C=O)s(50) + ϕ(Cα—C=O)(10) + ϕ(Cα—C=N)(7)+ ϕ(N—Cα—Cβ)(5)	450		ϕ(N—C=O)s(81)
111	0.72	ϕ(Cα—C=N)(19) + ϕ(C=N—C)(18) + τ(C=N)(10)+ ϕ(N—Cα—C)(10) + ϕ(N=C=O)(7) + ϕ(N—Cα—Cβ)(5)+ ϕ(Cα—C=O)(5)	108	0.85	τ(C—N)s(47) + ϕ(Cα—C=N)(9) + ϕ(Cβ—Cα—Cβ)(7)+ τ(C=N)(6)
106		τ(C—N)s(93)	104		τ(C—N)s(47) + ϕ(Cα—C=N)(9) + ϕ(C=N—C)(7) τ(C=N)(6) + ϕ(N—Cα—C)(5)

Note: All frequencies are in cm^{-1}.

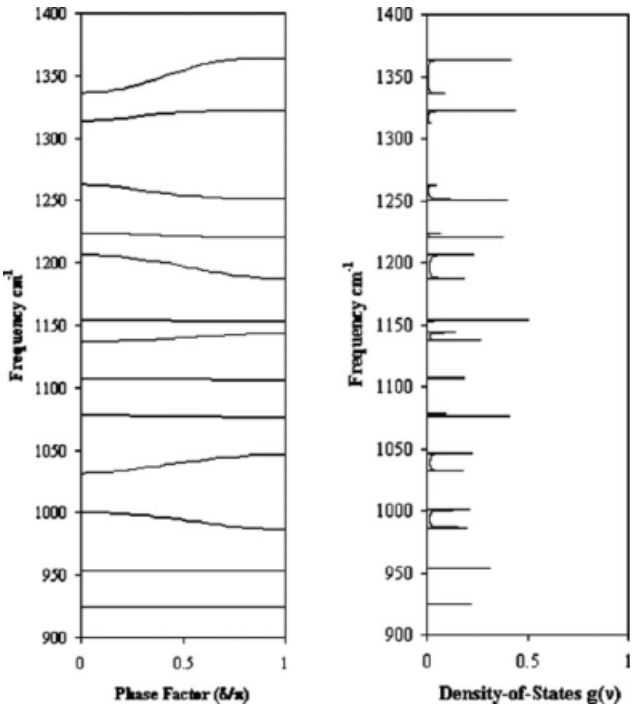

Figure 3 (a) Dispersion curves of poly(L-glutamine) (1400–900); (b) density-of-states of poly(L-glutamine) (1400–900).

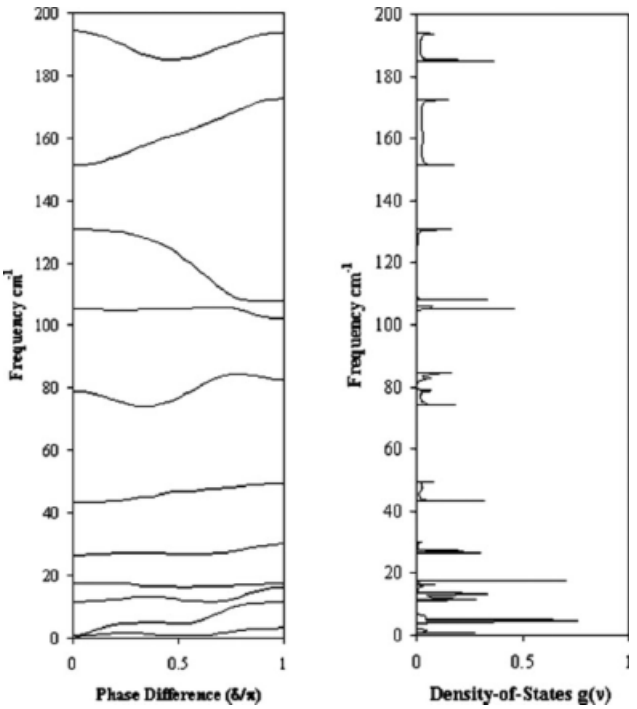

Figure 5 (a) Dispersion curves of poly(L-glutamine) (below 200); (b) density-of-states of poly(L-glutamine) (below 200).

contribution of angle bend of (C=N—H) comes in and becomes zero at $\delta = 0.70$. It is seen at $\delta = 0.75$ that the contribution of angle bend of (N—Cα—C) and (N=C=O) becomes zero while the contribution of (Cβ—Cα—Cβ) comes in. For the 105 cm^{-1} mode, we see that it is purely the contribution of torsion of C—N of the side chain, but it increases with the increase in the delta values. At $\delta = 0.80$, we see that the contribution of the angle bend of (Cα—C=N) and (C=N—C) comes in. It is also seen at $\delta = 0.95$ that the contribution of angle bend of (C=N—C) becomes zero and contribution of angle bend of (Cβ—Cγ—C) comes in. For the 79 cm^{-1} mode, we see that at $\delta = 0.30$ the contribution of angle bend of (Cα—C=N) and torsion (Cα—Cβ) becomes zero. Furthermore, at $\delta = 0.35$, the contribution of torsion of (Cγ—C) becomes zero and at $\delta = 0.45$ the contribution of wagging of CO comes in. It is also seen at $\delta = 0.50$ that the contribution of wagging of the N—H of side chain comes in and at $\delta = 0.75$ contribution of angle bend (C=N—C) comes in.

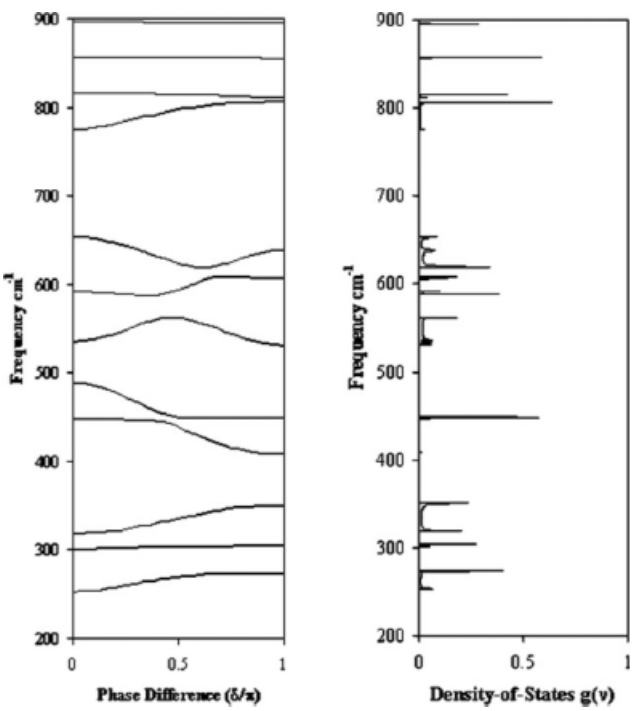

Figure 4 (a) Dispersion curves of poly(L-glutamine) (900–200); (b) density-of-states of poly(L-glutamine) (900–200).

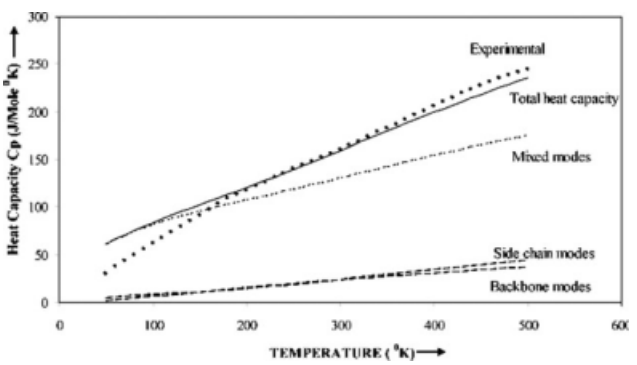

Figure 6 Heat capacity variation with temperature of poly(L-glutamine).

Density of states and heat capacity

The normalized density of states versus frequency plots obtained from the dispersion curves is given in Figures 3(b), 4(b), and 5(b). The peaks in the frequency distribution curves represent the frequencies of high density of states, which is supported by the observed frequencies in the same region.

We see from the frequency distribution curves that the heat capacity of PLGn has been calculated from 50 to 500 K. Our calculations of the heat capacity data are in good agreement with the reported data of ATHAS Data bank Update (1993) (Fig. 6). The divergence in two heat capacity data below 150 K is due to neglect of lattice modes that lie below this frequency. The heat capacity is also sensitive to these modes in this region. The contributions of the heat capacity are also calculated separately for the side chain, backbone, and mixed modes and are plotted in the same figure. It is clear that the major contribution comes from the side chain and mixed modes. The sum of these three contributions gives the total capacity. The use of a small scaling factor of 1.07 brings the calculated heat capacity data into full agreement with the experimental measurements. The scaling factor takes into account any constant error in experimental measurements that cause a constant shift of the experimental curve. The same can be said for the theoretical curve as well. The results show that the heat capacity is sensitive to the conformation of the chain, especially in the low-temperature region (<300 K).

It may be added here that the contribution from the lattice modes is bound to make a difference to the heat capacity because of its sensitivity to low frequency modes. However, so far we have solved the problem only for an isolated chain. The calculation of dispersion curves for a three-dimensional system is extremely difficult. Inter-chain modes involving hindered translatory and rotatory motion that appear and the total number of modes will depend on the contents of the unit cell. It would not only make the dimensionality of the problem prohibitive but also bring in an enormous number of interactions that are difficult to visualize, much less to quantify. Thus it makes the problem intractable. The inter-chain interactions contribute to lower frequencies. They are generally of the same order of magnitude as the weak intra-chain interactions. Their introduction would at best bring about crystal field splittings at the zone center or zone boundary, depending on the symmetry-dependent selection rules. However, the intra-chain assignments will remain by and large undisturbed. Thus, despite several limitations involved in the calculation of specific heat, the present work does provide a good starting point for further basic studies on thermodynamic behavior of polypeptides that go into well-defined conformations. Complete three-dimensional studies have been reported only on polyethylene and polyglycine, in which the unit cell is small. Other calculations with approximate inter-chain interactions as β sheets of polypeptides are confined to calculations of zone center and zone boundary frequencies alone by considering short segments and nearest neighbor interactions only. The present work goes beyond this and calculates the dispersion curves within the entire zone.

References

1. Prasad, O.; Tandon, P.; Gupta, V. D.; Rastogi, S. J Polym Sci Part B: Polym Phys 1996, 34, 1213.
2. Gupta, V. D.; Trevino, S.; Boutin, H. J Chem Phys 1968, 48, 3008.
3. Srivastav, S.; Tandon, P.; Gupta, V. D.; Rastogi, S.; Mehrotra, C. Polym J 1997, 29, 33.
4. Krishnan, M. V.; Gupta, V. D. Chem Phys Lett 1970, 7, 285.
5. Singh, R. D.; Gupta, V. D. Spectrochim Acta 1971, 27, 385.
6. Dwivedi, A. M.; Gupta, V. D. Chem Phys Lett 1972, 16, 909.
7. Gupta, V. D.; Singh, R. D.; Dwivedi, A. M. Biopolymers 1973, 12, 1377.
8. Krishnan, M. V.; Gupta, V. D. Chem Phys Lett 1970, 6, 231.
9. Burman, L.; Tandon, P.; Gupta, V. D.; Rastogi, S.; Srivastav, S.; Gupta, G. P. J Phys Soc Jpn 1995, 64, 327.
10. Gupta, A.; Tandon, P.; Gupta, V. D.; Rastogi, S.; Gupta, G. P. J Phys Soc Jpn 1995, 64, 315.
11. Burman, L.; Tandon, P.; Gupta, V. D.; Rastogi, S.; Srivastav, S. Polym J 1995, 27, 481.
12. Wunderlich, B.; Bu, H. S. Thermochim Acta 1987, 119, 225.
13. Bu, H. S.; Aycock, W.; Cheng, S. Z. D.; Wunderlich, B. Polymer 1988, 29, 1486.
14. Roles, K. A.; Wunderlich, B. Biopolymers 1991, 31, 477.
15. Roles, K. A.; Xenopoulos, A.; Wunderlich, B. Biopolymers 1993, 33, 753.
16. Available at: Muscleandstrength.com/supplements/glutamine.html.
17. Wilson, E. B.; Decius, J. C.; Cross, P. C. Molecular Vibrations: The Theory of Infrared and Raman Vibrational Spectra; Dover Publication: New York, 1980.
18. Higgs, P. W. Proc R Soc London 1953, 220, 472.
19. Tandon, P.; Gupta, V. D.; Prasad, O.; Rastogi, S.; Gupta, V. P. J Polym Sci Part B: Polym Phys 1997, 35, 2281.
20. Pan, M.; Verma, N.; Wunderlich, B. J Therm Anal 1989, 35, 955.
21. Srivastav, S.; Tandon, P.; Gupta, V. D.; Rastogi, S. Polymer 1996, 37, 5401.
22. Renugopalakrishnan, V.; Bhatnagar, R. S. J Am Chem Soc 1984, 106, 2217.
23. Bahuguna, G. P.; Tandon, P.; Gupta, V. D.; Rastogi, S.; Mehrotra, C. J Macromol Sci Phys 1997, 36, 535.
24. Barth, A. Biophys Mol Biol 2000, 74, 141.